Eur Biophys J (2004) 33: 50–58
DOI 10.1007/s00249-003-0341-8

ARTICLE

B. Manz · M. Hillgärtner · H. Zimmermann
D. Zimmermann · F. Volke · U. Zimmermann

Cross-linking properties of alginate gels determined by using advanced NMR imaging and Cu^{2+} as contrast agent

Received: 12 May 2003 / Revised: 1 July 2003 / Accepted: 1 July 2003 / Published online: 16 September 2003

Abstract The entrapment of enzymes, drugs, cells or tissue fragments in alginates cross-linked with Ca^{2+} or Ba^{2+} has great potential in basic research, biotechnology and medicine. The swelling properties and, in turn, the mechanical stability are key factors in designing an optimally cross-linked hydrogel matrix. These parameters depend critically on the cross-linking process and seemingly minor modifications in manufacture have a large impact. Thus, sensitive and non-invasive tools are required to determine the spatial homogeneity and efficacy of the cross-linking process. Here, we show for alginate microcapsules (between 400 μm and 600 μm in diameter) that advanced ^{1}H NMR imaging, along with paramagnetic Cu^{2+} as contrast agent, can be used to validate the cross-linking process. Two- and three-dimensional images and maps of the spin-lattice relaxation time T_1 of Ba^{2+} cross-linked microcapsules exposed to external Cu^{2+} yielded qualitative as well as quantitative information about the accumulation of Cu^{2+} within and removal from microcapsules upon washing with Cu^{2+} free saline solution. The use of Cu^{2+} (having a slightly higher affinity constant to alginate than Ba^{2+}) for gelling gave a complementary insight into the spatial homogeneity of the cross-linking process together with information about the mechanical stability of the microcapsules. The potential of this technique was demonstrated for alginates extracted from two different algal sources and cross-linked either externally by the conventional air-jet dropping method or internally by the "crystal gun" method.

Keywords NMR imaging · Alginate · Cross-linking agents · "Crystal gun" method · Diffusion · Mechanical stability

B. Manz · F. Volke
Arbeitsgruppe Magnetische Resonanz,
Fraunhofer-Institut für Biomedizinische Technik (IBMT),
66386 St. Ingbert, Germany

M. Hillgärtner · U. Zimmermann (✉)
Lehrstuhl für Biotechnologie, Biozentrum,
Universität Würzburg, 97074 Würzburg, Germany
E-mail: zimmerma@biozentrum.uni-wuerzburg.de
Tel.: +49 931 888 4508
Fax: +49 931 888 4509

H. Zimmermann
Arbeitsgruppe Tieftemperatur-Biophysik,
Fraunhofer-Institut für Biomedizinische Technik (IBMT),
66386 St. Ingbert, Germany

D. Zimmermann
Abteilung für Biophysikalische Chemie,
Max-Planck-Institut für Biophysik, 60439 Frankfurt, Germany

Introduction

Alginates are found in brown algae and in bacterial species (Rehm 2002). They represent a family of linear co-polymers consisting of (1–4)-linked β-D-mannuronic acid (M) and its C-5 epimer α-L-guluronic acid (G). The two monosaccharides are arranged in homopolymeric (poly-mannuronate or poly-guluronate) or heteropolymeric block structures. The M:G ratio and the percentage of the block structures depend on the algal source (McHugh 1987). The length of the polymeric chains can vary considerably. Most alginates exhibit extremely non-uniform broad molecular mass distributions. Accordingly, the intrinsic viscosity of a 0.1% w/v solution in distilled water can vary from 1 mPa s to 60 mPa s. The viscosity and the molecular mass distribution depend strongly on the input source of algal material and the extraction process but can be modified by changes in ionic strength (Zimmermann et al. 2000, 2003b). The alkali-, ammonium- and magnesium-alginates are soluble in water. However, alginates can be gelled by cross-linking with divalent or trivalent cations (for more details, see Haug and Smidsrød 1970). This property is used for entrapment of enzymes, drugs, cells and tissue pieces. Conventionally, cross-linking is achieved by dropping alginate/cell droplets into a medium containing Ca^{2+} or Ba^{2+}. Immobilization of biologically active material has found a broad range of applications in

basic research (e.g. stabilization of wall-less cells) and in a number of biophysical (sensor technology) and biotechnological applications (Chibata 1978; Cohen et al. 1991; Draget et al. 2002; Hartmeier 1986; Kailasapathy 2002; Laskin 1985; Schnabl and Zimmermann 1989; Tonnesen and Karlsen 2002). Ca^{2+} or Ba^{2+} cross-linked alginate microcapsules also provide a new strategy for transplantation of allo- and xenografts without immunosuppressive therapy (Hasse et al. 1997; Hunkeler et al. 2001; Kühtreiber et al. 1999; Mullen et al. 2000). When enclosed in an alginate microcapsule, cells and tissues are protected against the immune response of the host while transfer of nutrients and oxygen and the release of therapeutic factors are not impeded. Despite much effort, progress in the field was hampered by variable stability of the microcapsules leading ultimately to transplant failure in animals and human beings (Kühtreiber et al. 1999; Mazaheri et al. 1991).

Major reasons for the instability of microcapsules include (i) concentration gradients of alginate polymers and/or of ingredients incorporated for stabilization (such as proteins) as well as (ii) the insufficient cross-linking within the core of the microcapsules. Polymer and protein concentration gradients arise from demixing and shrinking processes during droplet formation and gelling. They depend on many factors, such as gravity, alginate viscosity, molecular mass distribution, microcapsule size, the presence of non-gelling salts (e.g. NaCl) and the time of cross-linking (see also Thu et al. 2000). Optimum viability and/or functionality of entrapped wall-less cells as well as of other biologically active material are generally achieved when the external Ba^{2+} or Ca^{2+} concentrations are adjusted to 20 mM and the cross-linking time to 15 min. Higher concentrations of divalent cations or longer exposure times of the alginate droplets in the cross-linking solution considerably improve the homogeneous cross-linking of the capsule core, but are lethal to the incorporated biological material.

The above problems have been overcome by the production of ultra-high viscosity alginates (UHV alginates; viscosity of a 0.1% w/v solution in distilled water >30 mPa s; unpublished data) and by internal gelling of the alginate droplets. UHV alginates exhibit a uniform molecular mass distribution. They do not contain short polymeric alginate chains and the high viscosity prevents the built-up of concentration gradients during alginate droplet formation and cross-linking. Internal gelling achieves homogenous cross-linking throughout the microcapsule's interior by the injection of $BaCl_2$ or $CaCl_2$ crystals into the droplets before Ba^{2+} or Ca^{2+} is externally applied (so-called "crystal gun" method; Zimmermann et al. 2003a). However, the improved cross-linking leads to changes in the diffusion properties of the gel matrix. As shown for encapsulated islets (Schneider et al. 2003), the tight and narrow network can restrict the exchange of nutrients and oxygen between the encapsulated cells/tissue and the external medium as well as the release of insulin.

Diffusion within the alginate gel matrices can be enhanced by lowering the alginate concentration, but that may affect cross-linking of the polymeric chains and thus the swelling properties and stability of the microcapsules. This is a general problem of hydrogels, but particularly of alginates because of the variable M:G ratio. Additionally, the variable percentage of the block structures make predictions of microcapsule features even more difficult. Therefore, there is a great demand for non-invasive tools that allow rapid and accurate determination of the cross-linking features of alginates.

In this communication we will demonstrate that advanced ^{1}H NMR imaging techniques meet these requirements. Contrast agents were needed to visualize the alginate microcapsules because they consist of about 99% water.

Screening experiments showed that the signal intensities of the alginate polymeric chains were too low to be detectable even when H_2O was replaced by D_2O for microcapsule preparation. However, use of Cu^{2+} as a contrast agent yielded the information about the efficacy of the cross-linking process. Cross-linking could be visualized by replacement of Ba^{2+} by Cu^{2+} for gelling. The affinity constant of this ion to alginate is similar to that of Ba^{2+} (Smidsrød and Skjåk-Braek 1990). Complementary data about the inappropriate cross-linking of Ba^{2+} cross-linked microcapsules were obtained by studying the diffusion of external Cu^{2+} into the core of the microcapsules. Comparison of microcapsules made up of alginates from different algal sources and cross-linked by the conventional as well as by the "crystal gun" method revealed that this NMR technique allows routine evaluation of the alginate gelling.

Theoretical background of NMR imaging

A detailed description of the NMR technique can be found in a variety of textbooks (e.g. Abragam 1961; Ernst et al. 1987; Fukushima and Roeder 1981; Slichter 1990). The principle of magnetic resonance is based on the discovery that many nuclei carry a spin and have, therefore, a magnetic moment. If a sample with nuclear spins is placed inside a strong, external magnetic field, B_0, the interaction of the magnetic moment with B_0 causes the nuclear spins to line up, thus creating a small magnetization vector within the sample. This magnetization can be manipulated by the application of radio frequency (rf) pulses of a given intensity and duration. Upon application of an rf pulse the magnetization vector precesses around B_0 with its specific so-called Larmor frequency $\omega_0 = \gamma B_0$, where the constant of proportionality, γ, is termed the gyromagnetic ratio and is a fundamental property of the nucleus. For a Hydrogen nucleus (proton), γ has a value of 2.68×10^8 Hz T^{-1} (Abragam 1961; Ernst et al. 1987; Fukushima and Roeder 1981).

NMR imaging uses the fact that the Larmor frequency, ω, is proportional to the polarizing magnetic field. If in addition to the external magnetic field, B_0, a

uniform magnetic field gradient **G** is applied, the frequency, ω, experiences a spatial signature and is at the position **r** given by

$$\omega(\mathbf{r}) = \gamma(B_0 + \mathbf{r} \cdot \mathbf{G}) \quad (1)$$

This allows the acquisition of two- and three-dimensional images of the spin distribution $\rho(\mathbf{r})$ (Callaghan 1991; Mansfield and Morris 1982). Although complete information about the structure of the sample can only be extracted from three-dimensional images, it is sometimes advantageous to record a series of two-dimensional images. This is especially the case when the speed of image acquisition is important, e.g. in studies of dynamical processes as described here. Typical acquisition times are in the range of minutes for a two-dimensional and several hours for a three-dimensional image.

The relationship given in Eq. (1) represents an oversimplification, as it ignores all spin interactions except those with the polarizing field and the magnetic field gradient. While other effects, such as relaxations, complicate the situation, they also provide a means to apply additional contrast to the image during the acquisition.

There are two basic processes of relaxation, one of which involves an exchange of energy between the spins and the surrounding thermal reservoir (lattice), called spin–lattice relaxation, and one in which spins return to thermal equilibrium by interacting with each other, called spin–spin relaxation. The corresponding relaxation times are referred to as T_1 and T_2, respectively (Abragam 1961; Slichter 1990).

A difference in T_1 relaxation times of spins in a sample can be used for the selective suppression of undesired spin signals using a so-called "inversion recovery" pulse sequence (Callaghan 1991). An initial 180° rf pulse inverts the magnetization vector and then the spin–lattice relaxation proceeds for a time t_{ir}. The remaining magnetization is then called back using a 90° rf pulse. The signal intensity, S, is described by

$$S(t_{ir}) = S_0(1 - 2\exp(-t_{ir}/T_1)) \quad (2)$$

where S_0 is the signal intensity for fully relaxed spin system.

The cross-over through zero signal intensity at $t_{ir} = \ln(2)T_1$ can be exploited to suppress the signal of spins with a specific value of T_1.

A relaxation time weighting of the image intensity can be achieved by adjusting the delay times T_R and T_E. The repetition time T_R determines the degree to which the equilibrium magnetization is able to recover between pulse train repetitions, while the echo time T_E determines the degree of transverse magnetization decay at the image acquisition. These delays therefore result in an image sensitivity for T_1 and T_2, and the signal intensity at position **r** is given by (Callaghan 1991).

$$S(\mathbf{r}) = \left\{1 - \exp\left[-\frac{T_R}{T_1(\mathbf{r})}\right]\right\} \exp\left[-\frac{T_E}{T_2(\mathbf{r})}\right] \rho(\mathbf{r}) \quad (3)$$

A more quantitative approach is to measure spatially resolved maps of relaxation times, which is achieved by acquiring multiple images with variable values of T_R and T_E, followed by attenuation analysis according to Eqs. (2) and (3).

Materials and methods

Alginates

For extraction of alginate from the brown algae *Laminaria pallida* and *Lessonia nigrescens* algal material was freshly harvested from the sea at the coast of Namibia and Chile, respectively. Peeled, bacteria-free stipes were used. The purification procedure was performed as described elsewhere (Jork et al. 2000; Zimmermann et al. 2001). Briefly, the alginate was extracted with 50 mM EDTA solution followed by a filtration step. Then the alginate was precipitated with ethanol (37% v/v) and dissolved in 0.5 M KCl. The solution was subject to two further ethanol precipitations. The purified alginate was sterilized with ethanol, dried under sterile conditions and stored at 4 °C.

This extraction and purification regime resulted in ultra-high viscosity alginates (> 30 mPa s in the case of a 0.1% w/v alginate solution in distilled water). Various analytical assays and animal studies showed (Leinfelder et al. 2003; Zimmermann et al. 2000, 2003b) that the purified alginates were free of mitogenic, cytotoxic and apoptosis-inducing contaminants and thus of clinical grade (CG). These material are termed UHV/CG alginates to distinguish them from low-viscosity, impure, commercial alginates. The extracted alginates were denoted according to the original algal material (UHV_{Lam} and UHV_{Les}). Before use, the alginates were dissolved in sterile 0.9% NaCl solution at concentrations of 0.7% w/v (UHV_{Lam}) and 0.8% w/v (UHV_{Les}). These concentrations were found to be appropriate for maintenance of viability and function of entrapped cells (Schneider et al. 2003; Zimmermann et al. 2003a).

Microcapsules

For cross-linking of the alginate with Ba^{2+} and Cu^{2+} two different encapsulation methods were used. It should be noted that encapsulation was carried out under sterile conditions and that the various solutions were sterilized by filtration before use.

Conventional method

For the formation of empty alginate microcapsules an air-jet two-channel droplet generator was used. The inner channel (0.5 mm in diameter) contained the alginate solution, the second one fed the air supply into the nozzle. The injection rate of the alginate into the nozzle was controlled by an electric motor. Homogeneous alginate droplets with diameters of between 400 μm and 600 μm were generated by regulating the velocity of the co-axial air stream. The droplets entered a bath solution containing multivalent cations to induce cross-linking (so-called external gelling; for further details, see Jork et al. 2000).

"Crystal gun" method

The basic principle of this method was recently introduced by Zimmermann et al. (2003a). An air-regulated dental jet was mounted perpendicularly to the conventional droplet stream at about one third of the distance between the nozzle and the cross-linking solution. This dental jet produced an air stream containing tiny crystals of the cross-linking agent that penetrated the fluid and

elastic alginate droplets before coming in contact with the bath solution (so-called internal and external gelling). The crystals were heated at a temperature of 150°C for 2 h and stored under dry and sterile conditions before use. To avoid an increase in osmolality of the cross-linking solution due to the crystal stream, the dental jet was placed between two metal plates each with a circular aperture (11 mm in diameter) through which the droplets fell.

Cross-linking and post-treatment of the microcapsules

The bath solution contained 20 mM $CuSO_4$ or 20 mM $BaCl_2$. The osmolality of the solutions was adjusted to 290 mOsm by using appropriate amounts of NaCl. In the case of Ba^{2+} the pH was buffered to a value of 7.0 by addition of 5 mM histidine. Cross-linking with Cu^{2+} ions was performed at pH 5.2. After a cross-linking time of 15 min the microcapsules were washed three times with 0.9% NaCl solution before being transferred into fresh NaCl solution and stored at 4 °C until use. When Ba^{2+} ions were used as cross-linking agent the stability of the microcapsules was improved by addition of 10% fetal calf serum (FCS) to the alginate solution. Additionally, the cross-linked microcapsules were treated with 6 mM Na_2SO_4 saline solution for 30 min after the three washing steps to precipitate excess Ba^{2+} ions (for further details, see Hillgärtner et al. 1999). In the case of Cu^{2+} ions, FCS could not be used because of protein precipitation.

NMR images were recorded of Cu^{2+} cross-linked microcapsules that had been incubated in 0.9% NaCl solution for 11 days (UHV_{Les} alginate) and 22 days (UHV_{Lam} alginate). Before NMR imaging studies of Cu^{2+} ion diffusion into the core of Ba^{2+} cross-linked, protein-stabilized microcapsules, the material was kept in 0.9% NaCl solution for 19 days. Two-dimensional images and T_1 maps were recorded on about 200 microcapsules suspended in about 0.06 ml NaCl solution and placed into a NMR tube (inner diameter 4 mm). Data were acquired in the absence of Cu^{2+} and 90 min and 15 h after the addition of 0.06 ml of 15 mM $CuSO_4$ solution (adjusted to 290 mOsm with NaCl; T_1 value = 0.1 s) to the saline solution. Then a three-dimensional NMR data set of the capsule pellet was acquired before the microcapsules were washed with pure NaCl solution for three times followed by acquisition of two-dimensional images and T_1 maps.

Addition of Cu^{2+} resulted in a drop of the pH to about 4.4. To reveal pH effects, but also effects of the duration of the external gelling on the homogeneity of cross-linking, microcapsules made from 0.8% UHV_{Les} and 0.7% UHV_{Lam} were pre-cross-linked in 20 mM $BaCl_2$ saline solution at pH 7.0 for 15 min before incubation in 20 mM $BaCl_2$ solutions at pH 4.4 for a further 2 h. Other microcapsules were fabricated by external gelling for 15 min and 24 h and at pH 7.0 and 4.4. Microcapsules made in this way were then treated with Cu^{2+} as described above.

NMR imaging

All NMR experiments were carried out on a Bruker DMX400 NMR spectrometer (Bruker, Rheinstetten, Germany) with microimaging equipment. The spectrometer uses a vertical 9.4 T magnet operating at a proton resonance frequency of 400 MHz. The two-dimensional images were recorded using a standard spin-echo multislice pulse sequence with $T_E = 3.8$ ms, $T_R = 1$ s, a spatial resolution of 78 μm, and a slice thickness of 0.2 mm. T_1 maps were reconstructed from 11 individual images which were acquired after an initial 180° rf pulse; T_1 was obtained by variation of the delay time t_{ir} (range 10 ms to 2 s) between the rf pulse and image acquisition. The parameters S_0 and T_1 from Eq. (2) were then fitted to the data of each image voxel using the Levenberg–Marquard method (Press et al. 1988). Slice position and spatial resolution were identical with those of the two-dimensional images.

The three-dimensional T_1-weighted images were recorded using a spin-echo pulse sequence with an initial 180° rf pulse to invert the magnetization. The delay time t_{ir} was adjusted for each sample separately in order to suppress the background water signal. Typical experimental parameters were $T_E = 1.8$ ms, $T_R = 0.4$ s, $t_{ir} = 190$ ms, and the spatial resolution 39 μm in the three directions.

Results

Cross-linking with Cu^{2+}

Two-dimensional NMR images of microcapsules cross-linked with Cu^{2+} ions instead of Ba^{2+} yielded information about the insufficient cross-linking resulting from the conventional method. As shown in Fig. 1 Cu^{2+} cross-linked microcapsules incubated in 0.9% NaCl solution for up to 22 days, respectively, can clearly be distinguished from the external solution indicating that the Cu^{2+} concentration within the microcapsules is higher than outside. The two-dimensional images exhibited no significant differences in cross-linking between the conventional and the "crystal gun" method. However, the improved cross-linking throughout the microcapsules by the "crystal gun" method became quite obvious upon suppression of the proton signal of the external solution by applying an inversion recovery sequence. Typical microcapsule surfaces reconstructed

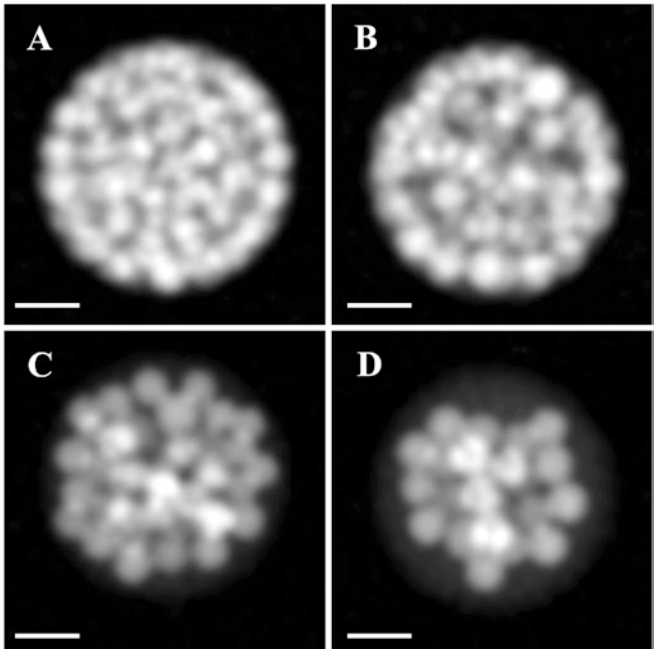

Fig. 1A–D Typical two-dimensional ^1H NMR images of a pellet of microcapsules (about 400 μm in diameter) cross-linked with Cu^{2+} ions using the "crystal gun" (**A** and **C**) and the conventional encapsulation method (**B** and **D**). The microcapsules in (**A**) and (**B**) were made up of 0.7% UHV_{Lam} alginate, the microcapsules in (**C**) and (**D**) of 0.8% UHV_{Les} alginate. UHV_{Lam} microcapsules were stored for 22 days, UHV_{Les} microcapsules for 11 days in 0.9% NaCl solution before use. Note that microcapsules when cross-linked with Cu^{2+} instead of Ba^{2+} can clearly be resolved because they exhibit significantly higher signals than the 0.9% NaCl solution. Bar = 1 mm

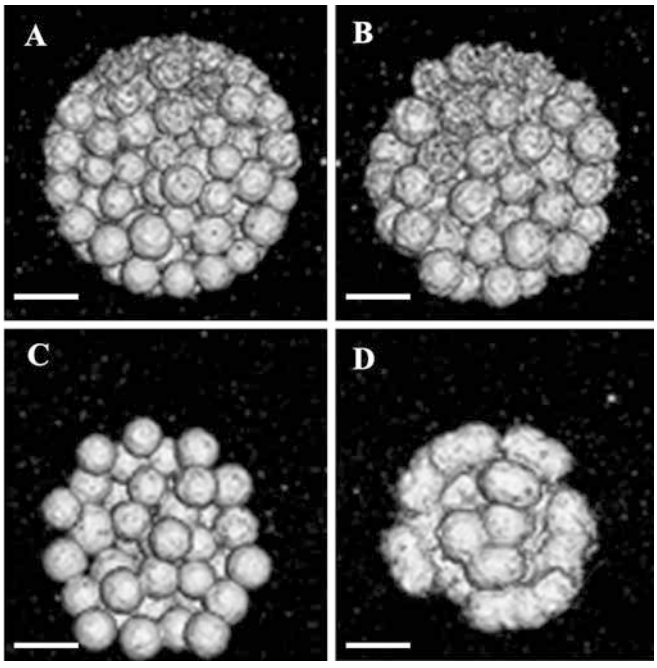

Fig. 2A–D Reconstructed surfaces deduced from three-dimensional NMR images of the microcapsules shown in Fig. 1. Note that microcapsules produced by using the "crystal gun" method (**A** and **C**) appear spherical and compact, whereas microcapsules made in the conventional way (**B** and **D**) were apparently quite deformed (**B**) or showed onset of deliquescence (**D**). Bar = 1 mm

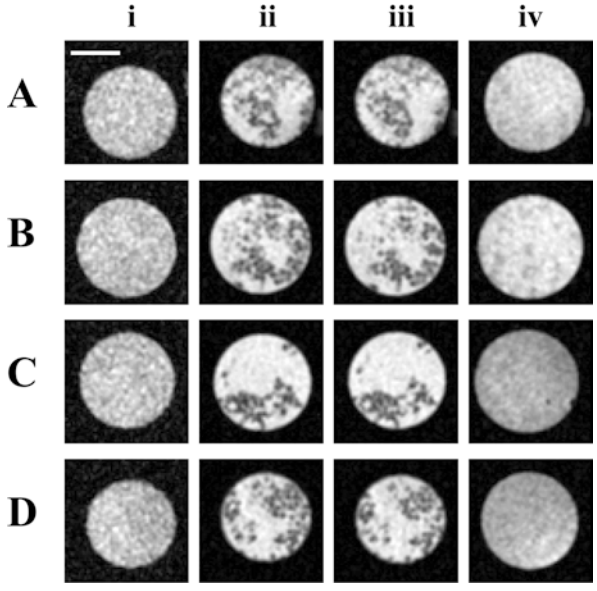

Fig. 3A–D, i–iv Typical two-dimensional ^{1}H NMR images of microcapsules (diameter about 400 μm) made of 0.7% UHV_{Lam} (**A** and **B**) and 0.8% UHV_{Les} alginate (**C** and **D**). Microcapsules were stabilized with 10% FCS and cross-linked with Ba^{2+} ions by using the "crystal gun" method (**A** and **C**) and the conventional, air-jet droplet method (**B** and **D**). The microcapsules were stored in a 0.9% NaCl solution for 19 days. For NMR measurements a pellet of microcapsules incubated in NaCl solution was placed into a NMR tube. Images were taken before (**i**), 90 min (**ii**) and 15 h (**iii**) after addition of 15 mM $CuSO_4$ and finally after replacing the Cu^{2+} ions by $CuSO_4$-free NaCl solution (**iv**). Note that the microcapsules can be only visualized as dark spheres in the presence of Cu^{2+} (**ii** and **iii**) and that the contrast between the capsules and the liquid surrounding disappears nearly completely after washing the microcapsules with pure 0.9% NaCl solution (**iv**). Bar (shown only in **A**, **i**) = 2 mm

from three-dimensional NMR images are depicted in Fig. 2. In the case of 0.7% UHV_{Lam} alginate microcapsules cross-linked by the "crystal gun" method (Fig. 2A) appeared less deformed than microcapsules produced by the conventional encapsulation method (Fig. 2B). This can be taken as evidence that internal gelling improves cross-linking and in turn mechanical stability. The benefits of injecting $CuSO_4$ crystals into the core of the microcapsules became even more evident in the case of 0.8% UHV_{Les} alginate (Fig. 2C). The microcapsules were spherical and appeared very compact, whereas UHV_{Les} microcapsules cross-linked only by external gelling are obviously less stable as indicated by the onset of deliquescence after 11 days of incubation (Fig. 2D).

Cross-linking with Ba^{2+}

We studied the diffusion of Cu^{2+} ions into the core of externally and internally gelled microcapsules to investigate whether the cross-linking procedure affects the permeability of microcapsules. The material had been cross-linked with Ba^{2+} at pH 7.0, and stabilized with 10% FCS and incubated in 0.9% NaCl solution for 19 days before use.

In Fig. 3A–D a typical series of two-dimensional images of microcapsules exposed to $CuSO_4$ in the NMR tube is shown. Before addition of $CuSO_4$ there was no contrast between capsules and medium (Fig. 3A–D, i). After an incubation time of 90 min a significant contrast could be detected due to differences in the T_1 values of the microcapsules and the surrounding medium (Fig. 3A–D, ii). The degree of contrast was apparently independent of the alginate (compare Fig. 3A and B, ii with Fig. 3C and D, ii) and of the encapsulation method (compare Fig. 3A and C, ii with Fig. 3B and D, ii). As shown in Fig. 3A–D, iii the contrast remained unchanged over an incubation time in $CuSO_4$-containing NaCl solution for 15 h. After removal of the Cu^{2+} ions by washing with $CuSO_4$-free NaCl solution (Fig. 3A–D, iv) the contrast between the microcapsule interior and the surrounding liquid was too weak for unambiguous visualization. Thus, in the light of two-dimensional images it was not possible to decide whether diffusion of Cu^{2+} into the core of the microcapsules was reversible or partly irreversible when using the two encapsulation methods.

However, T_1-weighted three-dimensional images gave clear-cut evidence that differences exist between encapsulation methods. Fig. 4 shows a typical two-dimensional slice of the three-dimensional data set performed on UHV_{Lam} alginate microcapsules incubated in $CuSO_4$-containing NaCl solution for about 17 h. As mentioned above, the slice thickness was 39 μm, i.e. much less than the diameter of the microcapsules (about 400 μm). It is evident that microcapsules made by

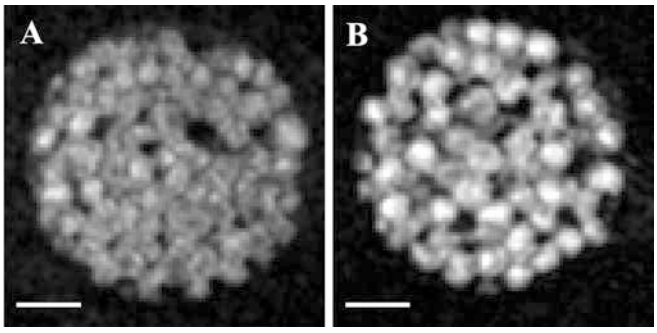

Fig. 4A–B Two-dimensional ^{1}H NMR images of UHV_{Lam} alginate microcapsules after incubation in $CuSO_4$-containing 0.9% NaCl solution for about 17 h. The images were obtained from a T_1-weighted three-dimensional data set, and the slice thickness was 39 μm. The microcapsules were prepared using the "crystal gun" (**A**) and the conventional (**B**) encapsulation method. Note that in both images a signal within the microcapsules is detectable, whereas signal intensity of the externally gelled microcapsules (**B**) is on average higher, indicating a higher internal Cu^{2+} concentration compared to the internally gelled microcapsules (**A**). Bar = 1 mm

injection of $BaCl_2$ crystals (Fig. 4A) exhibited on average less signal intensity (i.e. less internal Cu^{2+}) than microcapsules made in the conventional way (Fig. 4B).

The difference in Cu^{2+} uptake of the various alginate matrices could be more clearly resolved and also quantified by taking spatially resolved maps of T_1 values. Typical T_1 maps of UHV_{Lam} microcapsules made by the "crystal gun" method are depicted in Fig. 5A. After an incubation time of 90 min in the saline $CuSO_4$ solution (Fig. 5A, i) the spatially resolved T_1 maps revealed a value of less than 0.1 s in those regions of the NMR tube where microcapsules could be detected in the two-dimensional image (Fig. 3A, ii). This value was significantly lower than the T_1 value of the surrounding medium (0.2 s). A decrease in the T_1 value is expected when the Cu^{2+} ion concentration within the core of the microcapsules is higher than in the surrounding medium. Similar results were found for microcapsules incubated for 15 h (Fig. 5A, ii). Interestingly, upon replacement of the saline $CuSO_4$ solution by 0.9% NaCl solution T_1 values of 0.5–1.0 s were recorded homogeneously through the microcapsule suspension (Fig. 5A, iii). These values agreed quite well with the T_1 value of the pure NaCl solution (1.5 s) thus explaining why microcapsules were not visible. Obviously, most paramagnetic ions had been washed out of the microcapsules, excluding irreversible binding to the cross-linked network and/or diffusion restrictions within the alginate network.

Typical T_1 maps of UHV_{Lam} microcapsules made by using the conventional method are shown in Fig. 5B for incubation times of 1.5 h (Fig. 5B, i) and 15 h (Fig. 5B, ii) in $CuSO_4$-containing NaCl solution. At first glance, the data were comparable with those obtained for internally gelled UHV_{Lam} microcapsules (Fig. 5A, i), because the T_1 values of the microcapsules

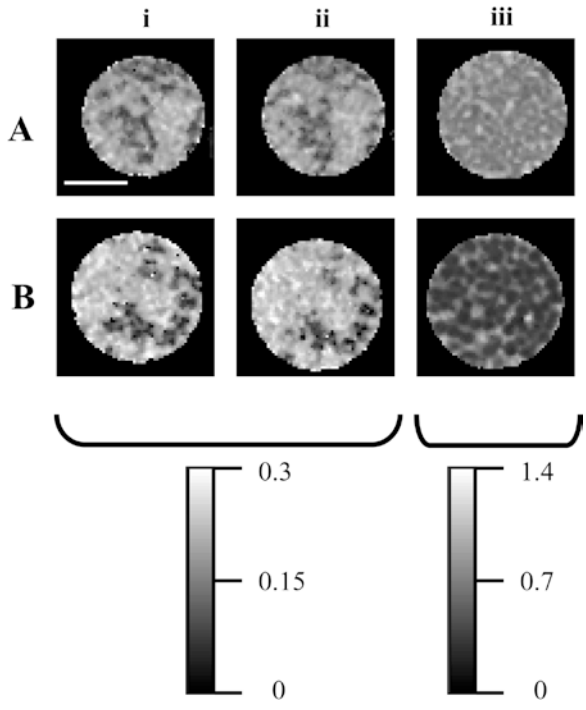

Fig. 5A–B, i–iii Spatially resolved ^{1}H NMR maps of the corresponding T_1 values of UHV_{Lam} microcapsules prepared using the "crystal gun" (**A**) and the conventional (**B**) encapsulation method. T_1 maps were recorded after 1.5 h (**i**) and 15 h (**ii**) upon $CuSO_4$ incubation and after washing the capsule pellet with $CuSO_4$-free NaCl solution (**iii**). The grayscale of the images represents the local value of T_1 given in seconds. Note that an increase in Cu^{2+} concentration lowers the T_1 values and vice versa. Bar (shown only in **A**, **i**) = 2 mm

were distinctively lower (0.1 s) than the T_1 values of the surrounding liquid (0.2–0.3 s; Fig. 5B, i). This indicates diffusion of Cu^{2+} into and accumulation of these ions within the microcapsules. The T_1 values also did not change over an incubation period of 15 h (Fig. 5B, ii). However, in contrast to microcapsules produced by the "crystal gun" method (Fig. 5A, iii) the difference in the T_1 values between the microcapsule interior and the surrounding remained after replacement of the saline $CuSO_4$ solution by 0.9% NaCl solution (Fig. 5B, iii). The T_1 values of the microcapsules only returned to near those of the surroundings when the microcapsules were kept in the saline solution for 19 h and then washed again with fresh 0.9% NaCl solution (data not shown).

In the case of 0.8% UHV_{Les} microcapsules technique Cu^{2+} release was nearly complete after the first washing procedure independent of encapsulation method (data not shown).

The difference between externally gelled UHV_{Lam} and UHV_{Les} might be due to insufficient equilibration of Ba^{2+} between the core of the charged matrix of UHV_{Lam} alginates and the surrounding medium. For this reason, experiments were performed on 0.7% UHV_{Lam} and 0.8% UHV_{Les} alginate microcapsules incubated in a saline 20 mM $BaCl_2$ solution at pH 7.0

for up to 24 h, before they were exposed to a saline $CuSO_4$ solution. Contrast and the T_1 values of the microcapsules were similar to those measured on microcapsules cross-linked for 15 min (Fig. 3B, ii and iii; Fig. 3D, ii and iii; Fig. 5B, i and ii; Fig. 5D, i and ii), but replacement of the $CuSO_4$ solution by NaCl solution resulted in the disappearance of the contrast of both UHV_{Lam} and UHV_{Les} microcapsules after the first washing procedure. Simultaneously, the T_1 values increased to the value of the surrounding medium indicating complete removal of the internal Cu^{2+} ions (data not shown). Neutralization of the carboxyl groups of the mannuronic and guluronic acid components by reduction of the pH of the cross-linking solution should also facilitate diffusion of external Ba^{2+} into the core of microcapsules made by UHV_{Lam} alginate. Consistent with this, microcapsules cross-linked by external Ba^{2+} for 15 min at pH 7.0 and then transferred to a saline 20 mM $BaCl_2$ solution of pH 4.4 for up to 2 h yielded similar results as long-term incubation in $BaCl_2$ solution at pH 7.0 for 24 h (data not shown). Similarly, cross-linking with Ba^{2+} at pH 4.4 for 15 min led to complete cross-linking of the core of the microcapsules as indicated by T_1 maps of the microcapsules after removal of the accumulated Cu^{2+} by washing with saline solution.

Discussion

The development of non-invasive imaging techniques for quality assessment of alginate microcapsules is crucial for applications in basic research, biotechnology and medicine. Maintenance of the network integrity while simultaneously allowing unrestricted diffusion of nutrients, oxygen and other factors are relevant to the viability, function, longevity of encapsulated cells, in particular for transplantation of allogeneic and xenogeneic (gene-manipulated) cells.

The efficacy of ^1H NMR imaging to monitor precisely relevant physico-chemical parameters of alginate microcapsules was demonstrated here by using two different cross-linking methods and alginates extracted from two different algal sources. Two-dimensional images show qualitatively that Ba^{2+} cross-linked microcapsules made by external gelling adsorbed more Cu^{2+} than microcapsules made by internal gelling. Selected slices of a full three-dimensional data set demonstrated quite clearly that external Cu^{2+} is not only adsorbed to the surface layer, but can diffuse into the core of the 400-μm thick microcapsules. More precise information about the cross-linking features of microcapsules could obviously be obtained from quantitative measurements of the spin–lattice relaxation time T_1 of microcapsules exposed to saline $CuSO_4$ solution. The T_1 values of microcapsules were below 0.1 s and thus lower than the T_1 value of the surrounding saline $CuSO_4$ solution (0.2 s). Since T_1 decreases with increasing Cu^{2+} concentration, this can be taken as clear-cut evidence of accumulation of Cu^{2+} within the alginate microcapsules. Accumulation was apparently independent of the employed encapsulation method and the alginate used. In the case of microcapsules cross-linked by the "crystal gun" method, consistent results were obtained for UHV_{Les} and UHV_{Lam} alginate microcapsules. Most of the accumulated Cu^{2+} could be rapidly removed by washing with saline solution. Thus, it is not very likely that Cu^{2+} was irreversibly bound to free carboxyl groups of the mannuronic and guluronic acid molecules (and to charged groups of FCS) or that Cu^{2+} has replaced bound Ba^{2+}. Formation of differently cross-linked layers due to alginate concentration gradients within or at the periphery of the microcapsule (Thu et al. 2000) can also obviously be excluded. Accumulation of Cu^{2+} within microcapsules made by the "crystal gun" method apparently occurred by unspecific adsorption to the alginate network or, more likely, to the charged groups of the FCS incorporated into the microcapsules for stabilization (see above).

At first glance, inconsistent results for the release kinetics of accumulated Cu^{2+} from UHV_{Les} and UHV_{Lam} alginate microcapsules were obtained when the conventional encapsulation method was used. Removal of Cu^{2+} was as rapid as that found for internal gelling when UHV_{Les} alginate was used. In contrast, the release of Cu^{2+} from UHV_{Lam} alginate microcapsules was considerably delayed. This delay can be straightforwardly explained by the assumptions that a tightly cross-linked peripheral layer is formed upon contact of UHV_{Lam} alginate with external Ba^{2+} and/or that the charged carboxyl groups of the polymeric chains restrict diffusion of the divalent cations into the core.

The finding that extension of the cross-linking time to 24 h at physiological pH values led to rapid and complete removal of Cu^{2+} from UHV_{Lam} alginate microcapsules is consistent with both assumptions. The NMR imaging results obtained for microcapsules made by cross-linking for 15 min at a pH of 4.4 suggested that charged groups apparently restricted diffusion of external Ba^{2+} and Cu^{2+}, respectively, into the core of the microcapsules. However, formation of a tightly cross-linked peripheral layer seems also to be involved as indicated by the NMR images of UHV_{Lam} alginate microcapsules cross-linked with external Cu^{2+} instead of Ba^{2+} for 15 min. These microcapsules exhibit distinctive deformations in contrast to microcapsules made by the "crystal gun" method (Fig. 2A and B). Deformations can be expected when the microcapsules consist of a liquid core surrounded by a tightly cross-linked layer. The NMR images of Cu^{2+} cross-linked microcapsules also represent an explanation for the rapid removal of Cu^{2+} from Ba^{2+} cross-linked microcapsules made up of UHV_{Les} alginate. As evidenced by Fig. 2D the insufficient cross-linking of the microcapsule core with external Cu^{2+} leads to disintegration of the microcapsules after about 2 weeks. Disintegration results from swelling and associated rupture of the ion bonds between the carboxyl groups of the polymeric chains (Zimmermann et al. 2000). If present, the tightly cross-linked peripheral layer will, therefore, be dissolved or torn, thus facilitating

the exchange of internal Cu^{2+} with the external NaCl in the washing solution.

The different response of UHV_{Lam} and UHV_{Les} alginate to external Ba^{2+} is quite surprising because both alginates exhibit a similar M:G ratio (about 70:30 and 60:40) and their viscosities are also comparable (around 30 mPa s). Thus, the number of charged carboxyl groups should be similar for both alginates. However, differences in the ratio of homopolymeric (poly-mannuronate or poly-guluronate) or heteropolymeric block structures may lead (together with the incorporated protein) to differences in the structural organization of the polymeric chains in the alginate droplets by hydrogen bonds and, in turn, to variations in the access of divalent cations to the charged carboxyl groups. The relatively broad size distributions (loosely associated with viscosity) and the associated size-dependent diffusion limitations may also add further problems (see above).

From this work it is obvious that such inherent problems of alginates and presumably of other hydrogels are absent when the "crystal gun" method is used. Internal gelling is clearly the method of choice for homogenous cross-linking of UHV alginate droplets at physiological pH values. Extended incubation times of up to 24 h or lowering the pH value of the cross-linking solution to 4.4 lead to similar results when gelling is performed externally, but these conditions are not beneficial for the viability and functionality of encapsulated cells.

It is also obvious that ^{1}H NMR imaging is a very useful and precise tool for monitoring the cross-linking features of alginates of different sources. The technique also offers the advantage that relatively few microcapsules from a batch are needed to resolve the spatial homogeneity of cross-linking as well as the permeability and accumulation properties of the alginate matrix for paramagnetic divalent cations or other paramagnetic ions and molecules. Thus, this technique can be used to investigate problems related to the manufacture of microcapsules, but also with long-term changes in the network integrity under in vitro and in vivo conditions. This technique can also be applied to study structural matrix changes induced by cryoconservation of microcapsules or encapsulated cells as increasingly required for biomedical applications. Progress in these fields is particularly expected if a quantitative index of cross-linking can be derived from the NMR image data. This seems possible if the resolution of the technique presented here is further enhanced.

Acknowledgements We are grateful to M. Behringer for his great help in the development of the "crystal gun" method. This work was supported by grants of the Bundesministerium für Bildung und Forschung (BMBF 0311588) to UZ, by BMBF grants (16SV1366/0 and 03N8707) to HZ and a research grant from IBMT to FV.

References

Abragam A (1961) The principles of nuclear magnetism. Clarendon Press, Oxford

Callaghan PT (1991) Principles of nuclear magnetic resonance microscopy. Clarendon Press, Oxford

Chibata I (1978) Immobilized enzymes. A Halsted Press Book. Kodansha, Tokyo and Wiley, New York

Cohen S, Bano MC, Chow M, Langer R (1991) Lipid–alginate interactions render changes in phospholipid bilayer permeability. Biochim Biophys Acta 1063:95–102

Draget KI, Smidsrød O, Skjåk-Braek G (2002) Alginates from Algae. In: Steinbüchel A, De Baets S, Vandamme EJ (eds) Biopolymers, vol 6, Polysaccharides II. Wiley-VCH, Weinheim, pp 215–244

Ernst RR, Bodenhausen G, Wokaun A (1987) Principles of nuclear magnetic resonance in one and two dimensions. Clarendon Press, Oxford

Fukushima E, Roeder SBW (1981) Experimental pulse NMR. A nuts and bolts approach. Addison-Wesley, Mass.

Hartmeier W (1986) Immobilisierte Biokatalysatoren. Springer, Berlin Heidelberg New York

Hasse C, Klöck G, Schlosser A, Zimmermann U, Rothmund M (1997) Parathyroid allotransplantation without immunosuppression. Lancet 350:1296–1297

Haug A, Smidsrød O (1970) Selectivity of some anionic polymers for divalent metal ions. Acta Chem Scand 24:843–854

Hillgärtner M, Zimmermann H, Mimietz S, Jork A, Thürmer F, Schneider H, Nöth U, Hasse C, Haase A, Fuhr G, Rothmund M, Zimmermann U (1999) Immunoisolation of transplants by entrapment in ^{19}F-labelled alginate gels: production, biocompatibility, stability, and long-term monitoring of functional integrity. Mat- wiss u Werkstofftech 30:783–792

Hunkeler D, Cherrington A, Prokop A, Rajotte R (2001) Bioartificial organs III. Tissue sourcing, immunoisolation and clinical trials. The New York Academy of Science, New York

Jork A, Thürmer F, Cramer H, Zimmermann G, Gessner P, Hämel K, Hofmann G, Kuttler B, Hahn HJ, Josimovic-Alasevic O, Fritsch KG, Zimmermann U (2000) Biocompatible alginate from freshly collected *Laminaria pallida* for implantation. Appl Microbiol Biotechnol 53:224–229

Kailasapathy K (2002) Microencapsulation of probiotic bacteria: technology and potentional applications. Curr Issues Intest Microbiol 3:39–48

Kühtreiber WM, Lanza RP, Chick WL (1999) Cell encapsulation technology and therapeutics. Birkhäuser, Boston, Mass.

Laskin AI (1985) Enzymes and immobilized cells in biotechnology. Benjamin/Cummings, London

Leinfelder U, Brunnenmeier F, Schiller J, Vásquez JA, Cramer H, Arnold K, Zimmermann U (2003) Highly sensitive cell assay for validation of purification regimes of alginates. Biomaterials 24:4161–4172

Mansfield P, Morris PG (1982) NMR imaging in biomedicine. Academic Press, New York

Mazaheri R, Atkison P, Stiller C, Dupré J, Vose J, O'Shea G (1991) Transplantation of encapsulated allogeneic islets into diabetic BB/W rats. Effects of immunosuppression. Transplantation 51:750–754

McHugh DJ (1987) Production and utilization of products from commercial seaweeds. Food and Agriculture Organization of the United Nations, Rome

Mullen Y, Maruyama M, Smith CV (2000) Current progress and perspectives in immunoisolated islet transplantation. J Hepatobiliary Pancreat Surg 7:347–357

Press WH, Teukolsky SA, Vetterling WT, Flannery BP (1988) Numerical Recipes in C. The art of scientific computing. Cambridge University Press, Cambridge, pp 683–688

Rehm BHA (2002) Alginates from bacteria. In: Steinbüchel A, Vandamme EJ, De Beats S (eds) Biopolymers, vol 5, Polysaccharides I. Wiley-VCH, Weinheim, pp 179–212

Schnabl H, Zimmermann U (1989) Immobilization of plant protoplasts. In: Bajaj YPS (ed) Biotechnology in agriculture and forestry, vol 8, Plant protoplasts and genetic engineering. Springer, Berlin Heidelberg New York, pp 63–96

Schneider S, Feilen P, Cramer H, Hillgärtner M, Brunnenmeier F, Zimmermann H, Weber MM, Zimmermann U (2003) Beneficial

effects of human serum albumin on stability and functionality of alginate microcapsules fabricated in different ways. J Microencapsulation 20:627–636
Slichter CP (1990) Principles of magnetic resonance. Springer, Berlin Heidelberg New York
Smidsrød O, Skjåk-Braek G (1990) Alginate as immobilization matrix for cells. Trends Biotechnol 8:71–78
Thu B, Gaserod O, Paus D, Mikkelsen A, Skjåk-Braek G, Toffanin R, Vittur F, Rizzo R (2000) Inhomogeneous alginate gel spheres: an assessment of the polymer gradients by synchrotron radiation-induced X-ray emission, magnetic resonance microimaging, and mathematical modeling. Biopolymers 53:60–71
Tonnesen HH, Karlsen J (2002) Alginate in drug delivery systems. Drug Dev Ind Pharm 28:621–630
Zimmermann U, Mimietz S, Zimmermann H, Hillgärtner M, Schneider H, Ludwig J, Hasse C, Haase A, Rothmund M, Fuhr G (2000) Hydrogel-based non-autologous cell and tissue therapy. Biotechniques 29:564–581
Zimmermann U, Cramer H, Jork A, Thürmer F, Zimmermann H, Fuhr G, Hasse C, Rothmund M (2001) Microencapsulation-based cell therapy. In: Reed G, Rehm HJ (eds) Biotechnology. Wiley-VCH, Weinheim, pp 547–571
Zimmermann H, Hillgärtner M, Manz B, Feilen P, Brunnenmeier F, Leinfelder U, Weber M, Cramer H, Schneider S, Hendrich C, Volke F, Zimmermann U (2003a) Fabrication of homogeneously cross-linked, functional alginate microcapsules validated by NMR-, CLSM- and AFM-imaging. Biomaterials 24:2083–2096
Zimmermann U, Leinfelder U, Hillgärtner M, Manz B, Zimmermann H, Brunnenmeier F, Weber M, Vásquez JA, Volke F, Hendrich C (2003b) Homogeneously cross-linked scaffolds based on clinical-grade alginate for transplantation and tissue engineering. In: Hendrich C, Nöth U, Eulert J (eds) Tissue engineering and cartilage replacement. Springer, Berlin Heidelberg New York, pp 77–86